Lit. Sem. 2010/7/14
Shunsuke Sakaoka (M2)

Cross-Linking System to Stabilize Alpha Helics Conformation in Short Peptides

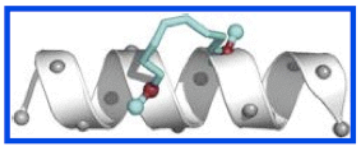

Contents

1 alpha helics conformation

Alapha helics, a common motif in the secondary structure of peptides, is right-handed coiled conformation.

- Every backbone N-H group donates a hydrogen bond to the backbone C=O group. (*i-I+4* hydrogen bonding)
- Each amino acid residues corresponds to a 100º trun in the helics.
- The pitch of the alpha-helics (the vertical distance between two consecutive turns of the helics) is 5.4Å.
- Residues in alpha helics typically adopt backbone (φ,ψ) dihedral angles around (-60º, -40º).

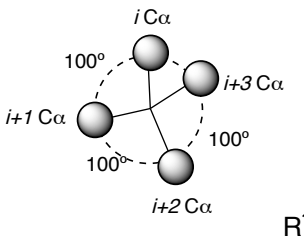

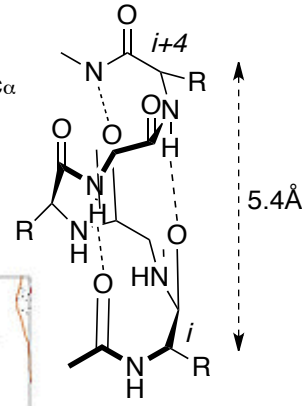

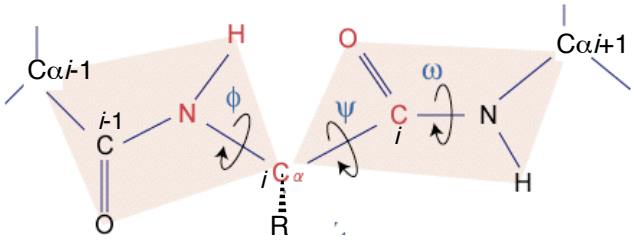

Ramachandran diagram

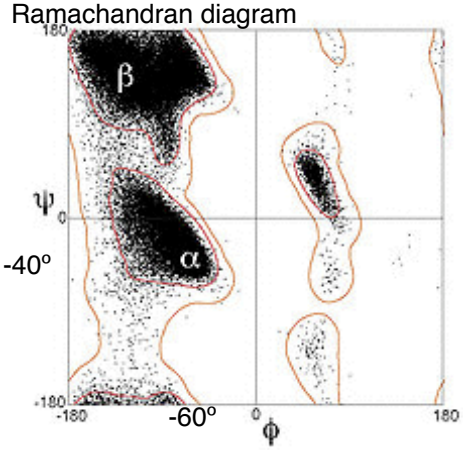

- Alpha helics is composed of 4 ~ 40 amino acid residues. (average 10 residues, 3 turns)
- Many of alpha helics are amphipathic. (e.g. alcohol dehydrogenase)

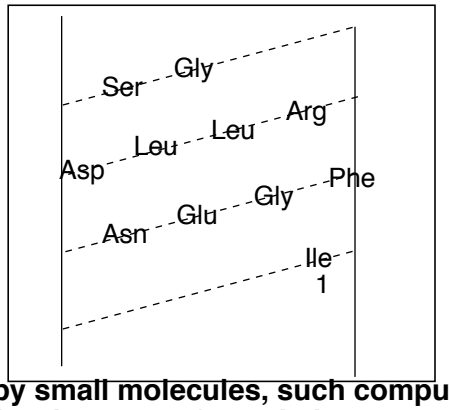

- Alpha helical sequences of ≤15 amino acids are estimated to account for ~30% of protein structure and frequently mediate biological processes through interactions with proteins, DNA or RNA.
- The folded states of most proteins are only ≤10 kcal/mol lower in energy than their unfolded states. (PNAS, 2006, 103, 16623)
  But short peptide sequences are usually unfolded in aqueous solution, awy from the helix stabilizing environments of proteins.

If short peptide alpha helics could be stabilized or mimicked by small molecules, such compunds might be valuable chemical or biological probes and lead to development of novel pharmaceuticals, vaccines, diagnostics, biopolymers and industrial agents.

• Circular Dichroism (CD) used to provide a quantitative measure of helical content.

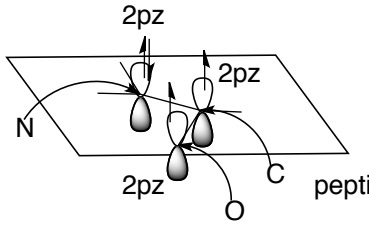

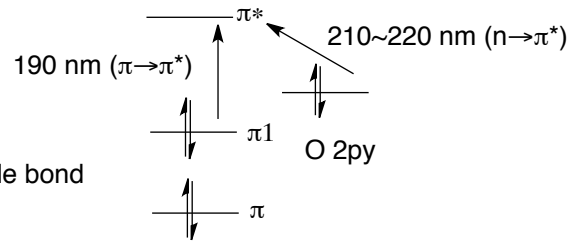

$[\theta(\lambda)] = \chi\alpha[\theta\alpha(\lambda)] + \chi\beta[\theta\beta(\lambda)] + \chi rc[\theta rc(\lambda)]$

$[\theta\alpha(\lambda)]$, $[\theta\beta(\lambda)]$,$[\theta rc(\lambda)]$; 2次構造が既知のポリペプチド鎖のα, β, rc構造に対する[θ]

$\chi\alpha,\chi\beta,\chi rc$; それぞれの存在割合

$$\text{alpha helix}(\%) = \frac{[\theta]_{208nm}+4000}{-33000+4000} \times 100$$

Alanine	Ala	A	Tyrosine	Tyr	Y
Lysine	Lys	K	Tryptophan	Trp	W
Aspartic acid	Asp	D	Threonine	Thr	T
Glutamic acid	Glu	E	Valine	Val	V
Asparagine	Asn	N	Histidine	His	H
Ariginine	Arg	R	Phenylalanine	Phe	F
Isoleucine	Ile	I	Proline	Pro	P
glycine	Gly	G	Methionine	Met	M
Glutamine	Gln	Q	Leucine	Leu	L
Cystein	Cys	C			
Serine	Ser	S			

Ala; CH_3 Glu; $(CH_2)_2CO_2H$
Lys; $(CH_2)_4NH_2$
Asp; CH_2CO_2H

2. some strategies to stabilize alpha helics conformation

2-1 Metal chelation

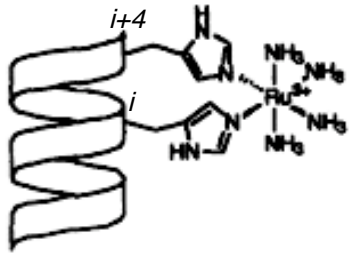

Peptide: Ac-AEAAAKEAAAKHAAAHA-NH_2

Figure 20 Binding of Ru(III) by His^{142}

M. Ghandiri JACS. 1990, 112, 9633
Rev) Tetrahedron 1999, 55, 11711

2-2-Template

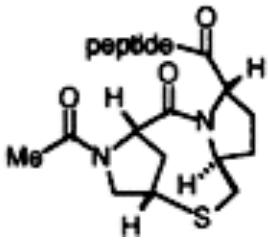

Template

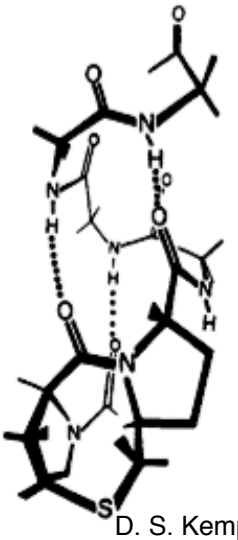

D. S. Kemp et al. JOC, 1991, 56, 672

2-3 Hydrogen-Bond Surrogate

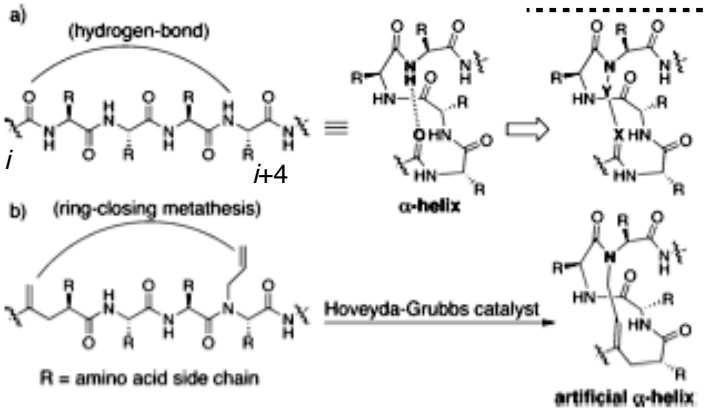

Paramijit S. Arora et al. JACS. 2004, 126, 12252

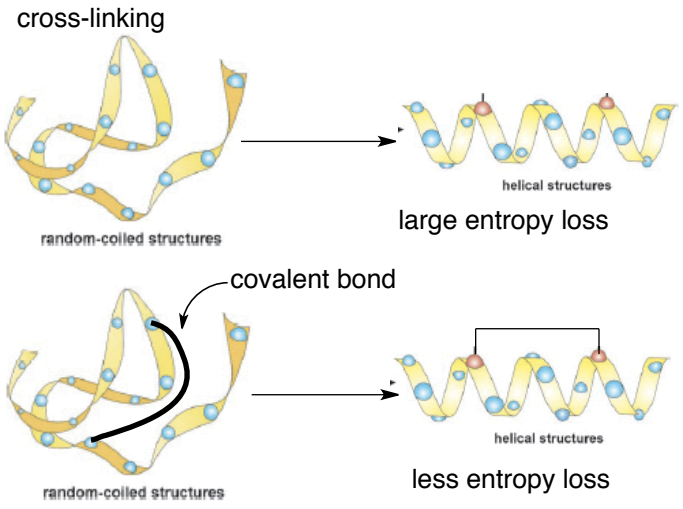

3 cross-linking with lactam bridge

Taylor, J. W. JACS, 1990, 112, 6046
Taylor, J. W, JACS, 1992, 114, 6966

3-1-1 design

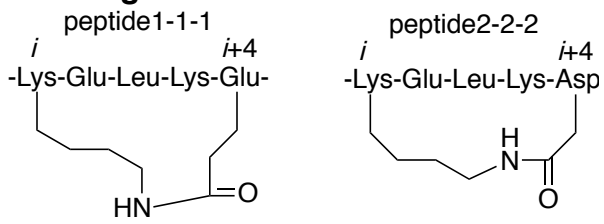

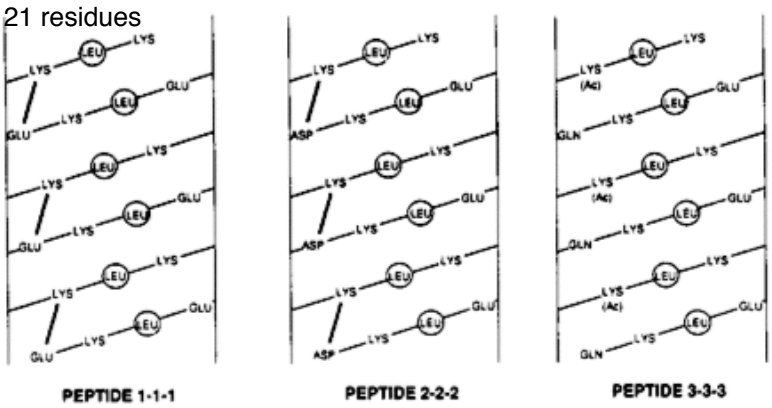

Figure 1. Helical net diagrams of the synthetic model amphiphilic α-helical peptides in this study.

3-1-2 synthesis of peptide 1-1-1

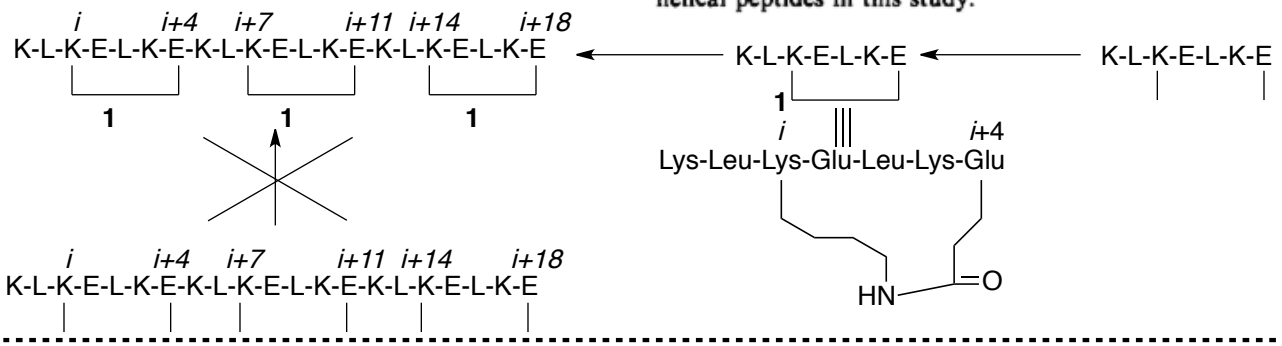

Synthesis of 1 (K-L-K-E-L-K-E)

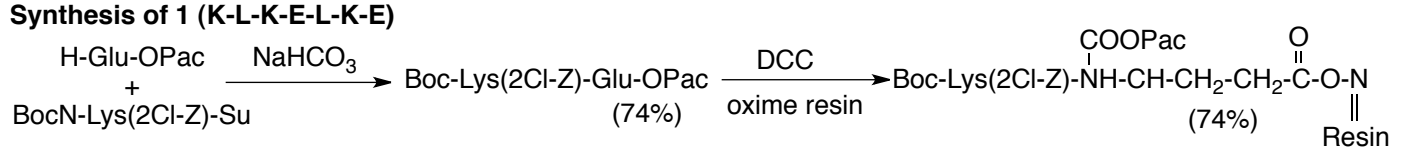

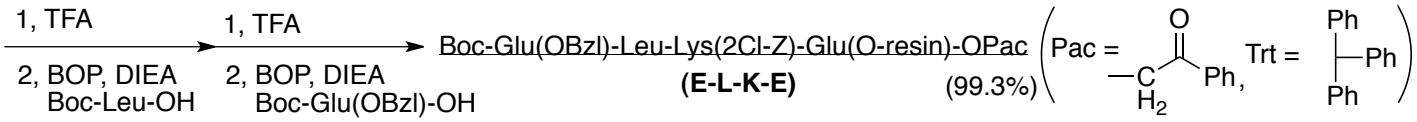

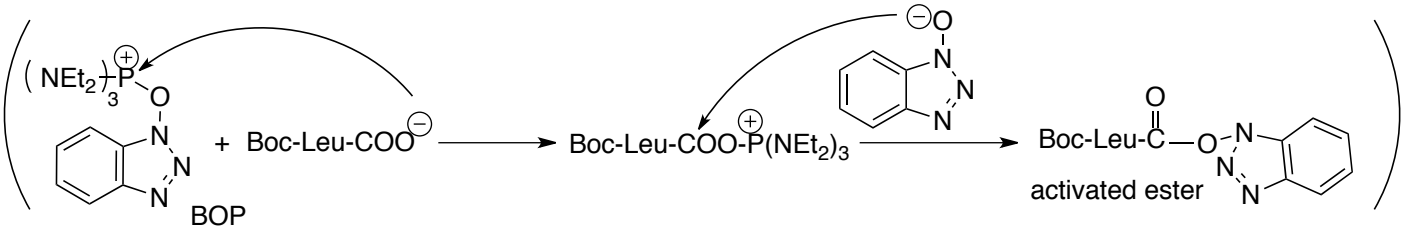

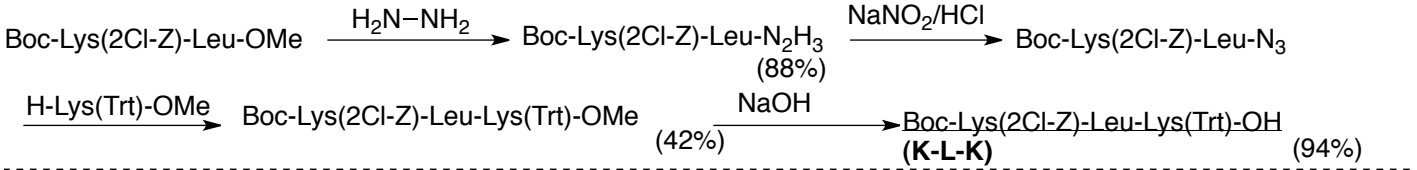

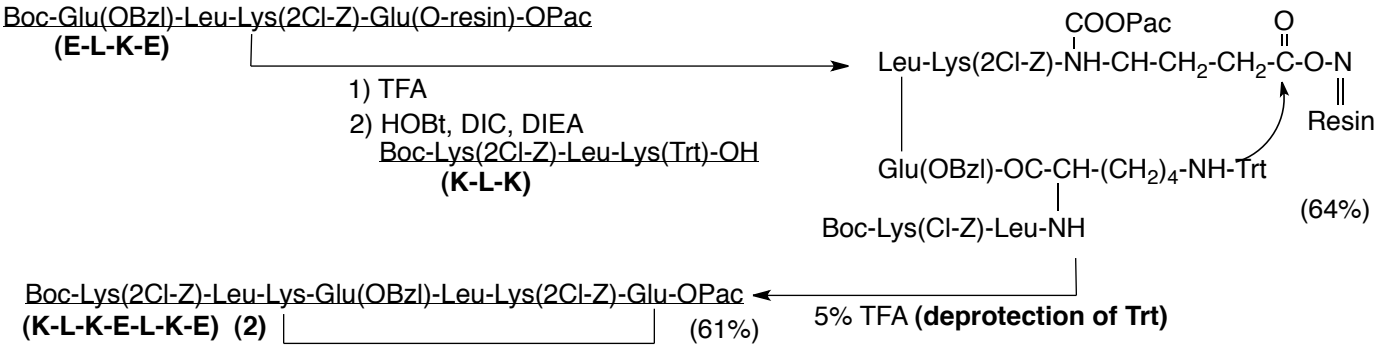

peptide-peptide coupling (DIC/HOBt)

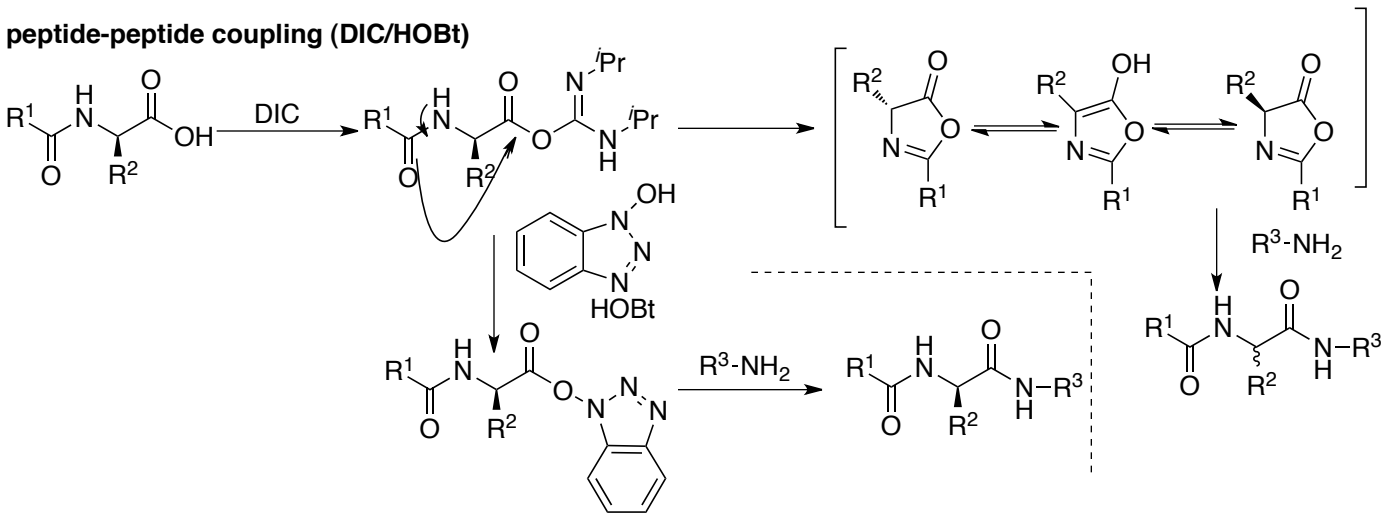

synthesis of 1-1-1

Scheme II. Synthesis of **1–1–1** by Segment Condensation[a]

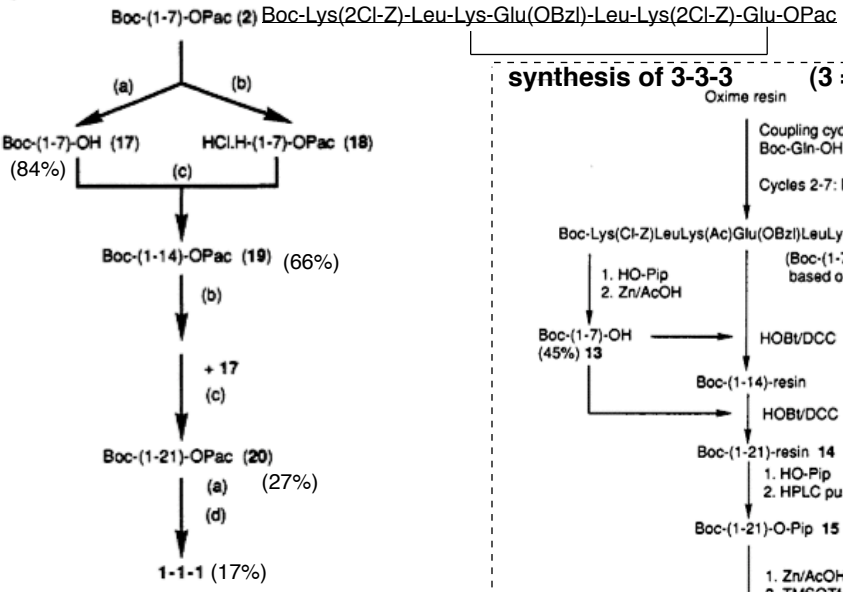

[a](a) Zn/AcOH; (b) TFA followed by HCl/dioxane; (c) HOBt/DCC; (d) TMSOTf + thioanisole in TFA.

synthesis of 3-3-3 (3 = Lys-Leu-Lys-Glu-Leu-Lys-Gln)

11→13

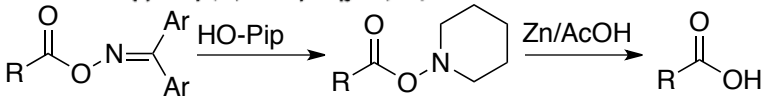

ref. JOC, 1983,48,678

3-1-3 CD spectra

CD spectra of 1-1-1, 2-2-2, 3-3-3

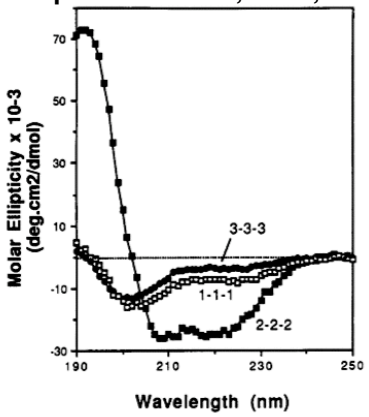

Figure 2. CD spectra of model peptides in aqueous 10 mM phosphate buffer, pH 7.0, at 25 °C: **1-1-1**, 40 μM (□); **2-2-2**, 30 μM (■); and **3-3-3**, 54 μM (●).

Cross-linking through Lys-Asp could stabilize alpha-helics in 21 residues peptide.

Cross-linking length is important?

Effect of TFE on helix formation

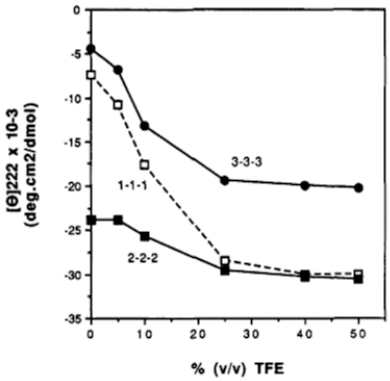

Figure 4. Effect of TFE on helix formation of synthetic peptides. Increasing proportions of TFE (%, v/v) were added to peptide solutions in aqueous 10 mM phosphate buffer, pH 7.0, at 25 °C and $[\theta]_{222}$ was monitored: **1-1-1**, 40 μM (□); **2-2-2**, 30 μM (■); **3-3-3**, 54 mM (●).

3-2 single turn peptide alpha helices

Nicholas E. Shepherd and David P. Fairlie JACS, 2005, 127, 2974

3-2-1 design

i *i+4*
Y/X-Z-Z-Z-X/Y ⟹ single turn alpha helics ??

X = Lys or Orn (Orn side chain; $-CH_2-CH_2-CH_2-NH_2$)
Y = Asp or Glu
Z = any amno acids

3-2-2 solid phase peptide synthesis (Fmoc protocol)

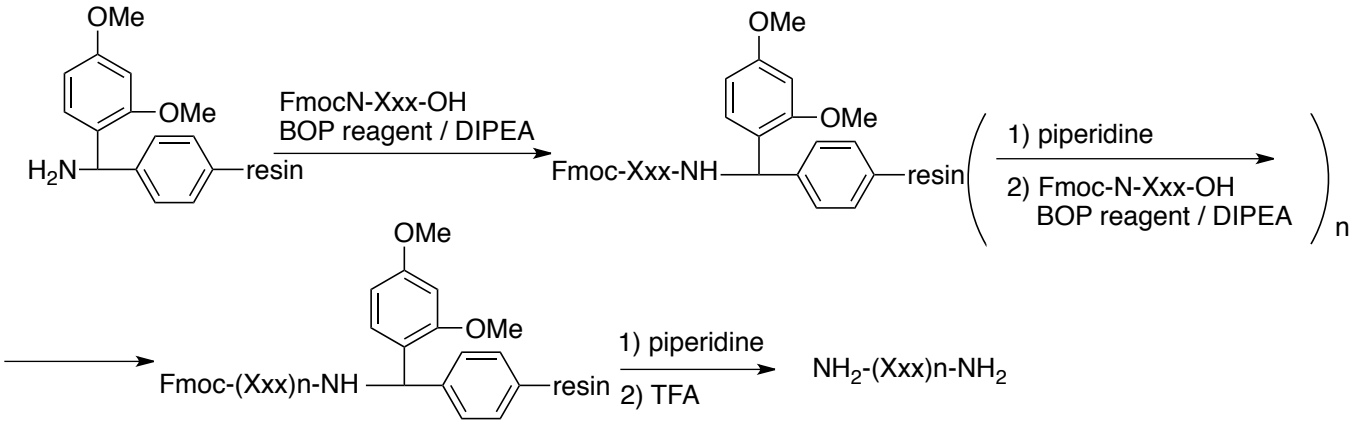

• Some Resins are used. Such as

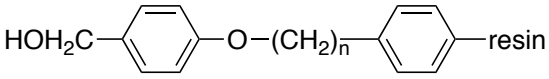

• Acids are not used except final step (cleavage from resin).

Side chains are protected with O^{t}Bu (for Asp, Glu), Boc (for Lys, Ser and His),Mtr, Pmc (for Arg) and so on which can be deprotected with TFA.

Mtr; 4-methoxy-2,3,6-trimethylbenzenesulfonyl

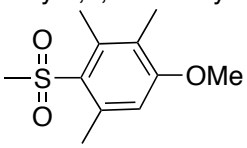

Pmc; 2,2,5,7,8-pentamethylchroman-6-sulfonyl

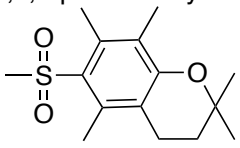

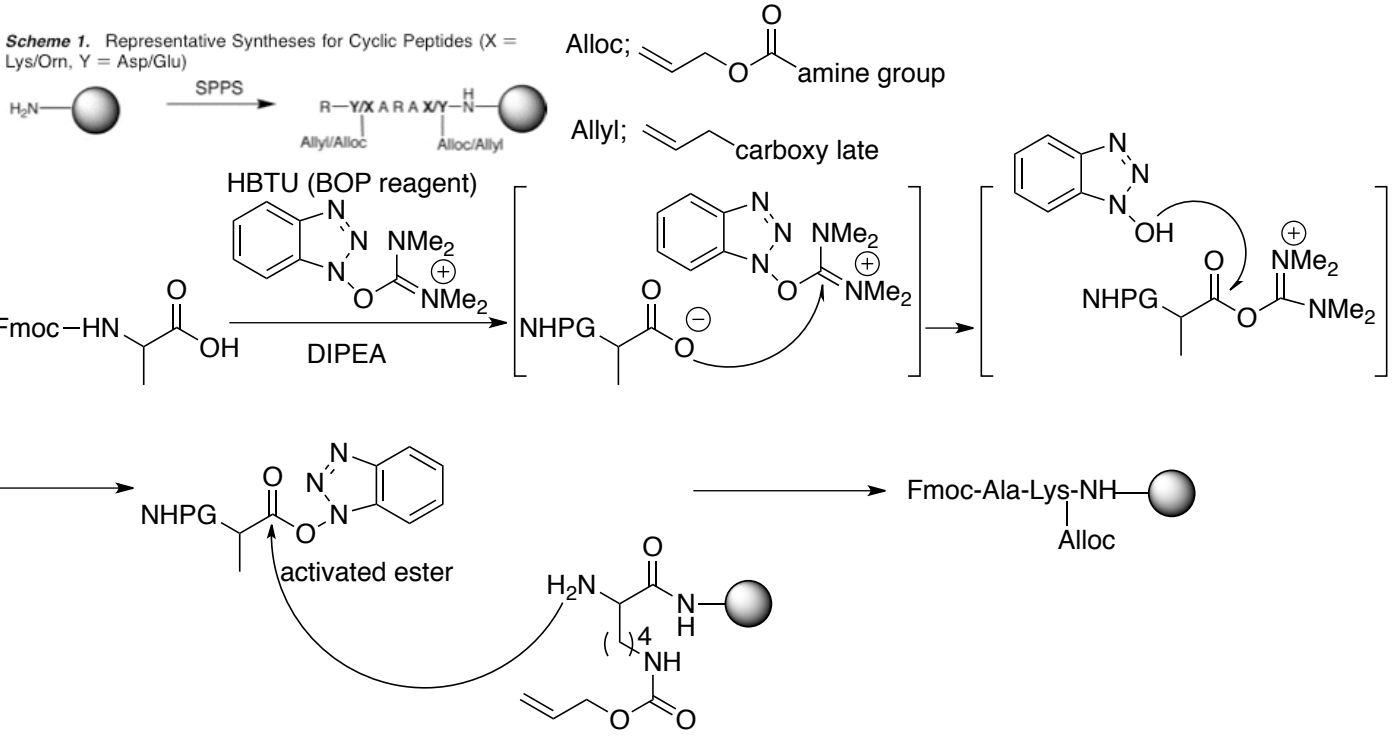

Scheme 1. Representative Syntheses for Cyclic Peptides (X = Lys/Orn, Y = Asp/Glu)

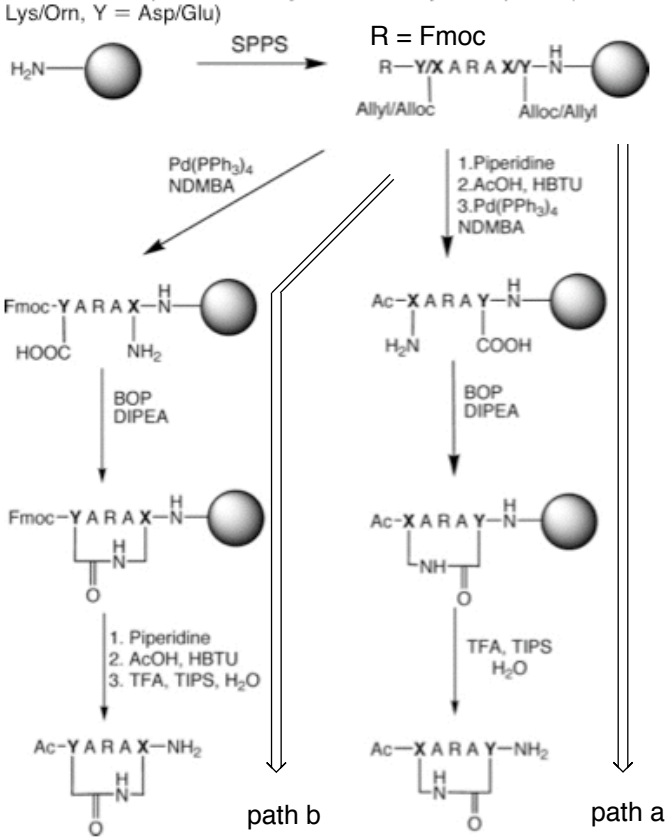

path a; Fmoc-K/O-A-R-A-D/E-NH-resin
path b; Fmoc-D/E-A-R-A-K/O-NH-resin

When Fmoc-D/E-A-R-A-K/O-NH- was cyclized through path a, some side reactions occurred.

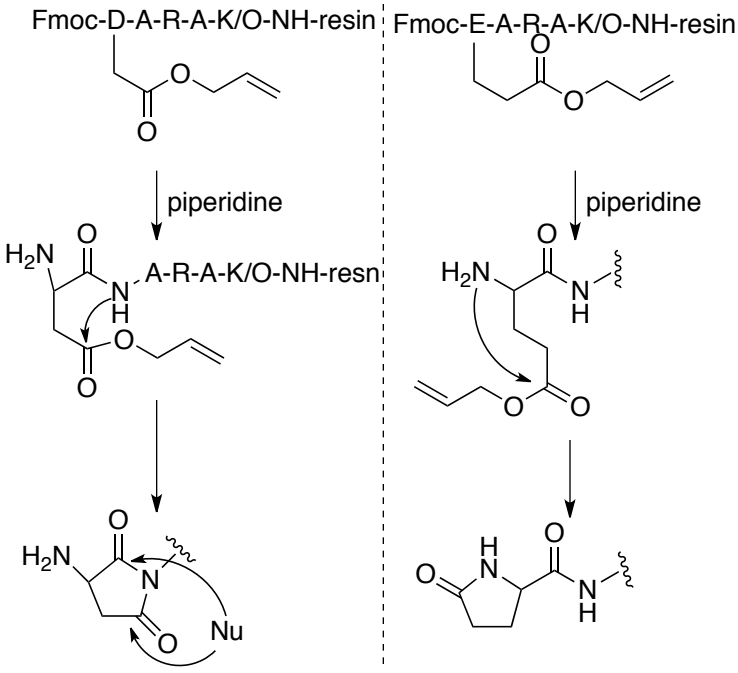

Thanks Dr. Nich.

3-2-3 result

CD-spectra-1 Ac-(cyclo-1,5)-[X/Y-ARA-Y/X]

Table 1. Molar Elipticities ([θ] deg cm^2 dmol^{-1} residue^{-1}) at λ = 215, 207, and 190 nm, Ratios of Elipticites at 215/207 nm, and Percentage Helicity for Peptides **1**−**12** in 10 mM Phosphate Buffer (pH 7.4, 25 °C)

peptide	$[\theta]_{215}$	$[\theta]_{207}$	$[\theta]_{190}$	$\theta_{215}/\theta_{207}$	relative helicity[c]
Ac-(cyclo-1,5)-[**K**ARA**E**]-NH$_2$ (**1**)	−1068	−3393	−10611	0.31	0.08
Ac-(cyclo-1,5)-[**E**ARA**K**]-NH$_2$(**2**)	−7430	−12803	20735	0.58	0.58
Ac-(cyclo-1,5)-[**K**ARA**D**]-NH$_2$ (**3**)	−12757	−12211	38300	1.04	1.00
Ac-(cyclo-1,5)-[**D**ARA**K**]-NH$_2$ (**4**)	−7723	−10705	15600	0.72	0.60
Ac-(cyclo-1,5)-[**O**ARA**D**]-NH$_2$ (**5**)	92	−2077	−4613	−0.04	0
Ac-(cyclo-1,5)-[**D**ARA**O**]-NH$_2$ (**6**)	−4671	−9748	−6954	0.48	0.37
Ac-(cyclo-1,5)-[**O**ARA**E**]-NH$_2$ (**7**)	741	−3368	−16228	−0.22	0
Ac-(cyclo-1,5)-[**E**ARA**O**]-NH$_2$ (**8**)	2442	−1917	−11256	−1.27	0
Ac-KARAD-NH$_2$ (**9**)	−524	−5555	−7372	0.09	0.04
Ac-(cyclo-1,5)-[**K**ARA**D**]-OH (**10**)	207	−5643	−13953	−0.04	0
a	−625	−3195	−2659	0.20	0.06
H-(cyclo-1,5)-[**K**ARA**D**]-NH$_2$ (**11**)	−812	−2228	1355	0.36	0.06
b	−2590	−3327	8452	0.78	0.2
H-(cyclo-1,5)-[**K**ARA**D**]-OH (**12**)	−1033	−5737	−4966	0.18	0.08

[a] In 0.01 M HCl pH 2. [b] In 0.001 M NaOH pH 10. [c] $[\theta]_{215}$ (**3**)/$[\theta]_{215}$ (**x**) refer to "Quantitation of Helicity" section.

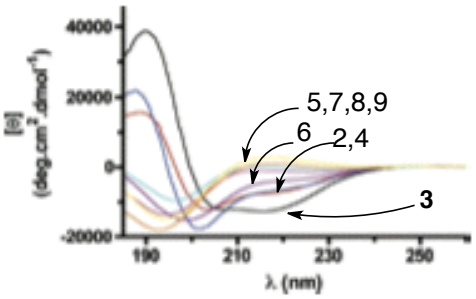

Figure 2. CD spectra of cyclic pentapeptides **1** (pink), **2** (blue), **3** (black), **4** (red), **5** (aqua), **6** (purple), **7** (orange), and **8** (yellow) in 10 mM phosphate buffer (pH 7.4, 25 °C).

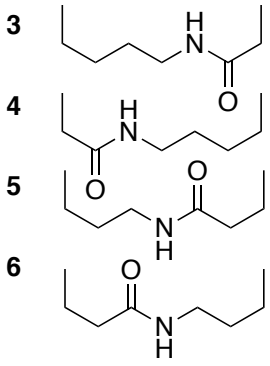

CD-spectra-2 Ac-(cyclo-2,6)-R[K-ZZZ-D] (helics dependence on sequences)

Table 2. Molar Elipticities ([θ] deg cm^2 dmol^{-1} residue^{-1}) at λ = 215, 207, and 190 nm, Ratios of Elipticites at 215/207 nm, and Percen Helicity for Cyclic Peptides **13**−**21** in 10 mM Phosphate Buffer pH 7.4 at 25 °C

peptide	$[\theta]_{215}$	$[\theta]_{207}$	$[\theta]_{190}$	$\theta_{215}/\theta_{207}$	relative helicity[a]
Ac-(cyclo-2,6)-R[**K**AAAD]-NH$_2$ (**13**)	−13 537	−13 684	39 352	0.99	0.91
Ac-(cyclo-2,6)-R[**K**ALAD]-NH$_2$ (**14**)	−14 798	−15 165	46 621	0.98	1.00
Ac-(cyclo-2,6)-R[**K**AMAD]-NH$_2$ (**15**)	−11 853	−12 296	38 464	0.96	0.80
Ac-(cyclo-2,6)-R[**K**AQAD]-NH$_2$ (**16**)	−11 394	−12 279	36 865	0.93	0.84
Ac-(cyclo-2,6)-R[**K**AFAD]-NH$_2$ (**17**)	−8644	−9087	27 718	0.95	0.76
Ac-(cyclo-2,6)-R[**K**AGAD]-NH$_2$ (**18**)	−4874	−7678	10 036	0.63	0.32
Ac-(cyclo-2,6)-R[**K**GSAD]-NH$_2$ (**19**)	−4810	−6975	12 831	0.69	0.32
Ac-(cyclo-2,6)-R[**K**SSSD]-NH$_2$ (**20**)	−4432	−8017	6827	0.55	0.30
Ac-(cyclo-2,6)-R[**K**GGGD]-NH$_2$ (**21**)	−2131	−4868	−1593	0.44	0.14

Rank order of helical propencities
(rev. Teterahedron, 1999,55,11711)

AQ/AK	ΔΔG kcal mol^{-1}	AXA	ΔΔG kcal mol^{-1}	T4 lysozyme	ΔΔG kcal mol^{-1}
Ala	-1.88	Ala	-1.05	Ala	-0.96
Arg	-1.67	Glu$^-$	-0.84	Leu	-0.92
Leu	-1.60	Leu	-0.69	Met	-0.86
Lys	-1.52	Ile	-0.67	Ile	-0.84
Met	-1.37	Arg	-0.64	Gln	-0.80
Gln	-1.31	Met	-0.53	Arg	-0.77
Glu$^-$	-1.20	His	-0.51	Lys	-0.73
Ile	-1.18	Lys	-0.47	Tyr	-0.72
Tyr	-1.3 to -1.1	Val	-0.32	Val	-0.63
Ser	-1.10	Ser	-0.29	Trp	-0.58
His	-1.07	Asp$^-$	-0.27	Phe	-0.59
Cys	-1.06	Gln	-0.25	His	-0.57
Asp$^-$	-1.00	Asn	-0.20	Thr	-0.54
Asn	-0.99	Thr	-0.17	Glu$^-$	-0.53
Trp	-1.1to-0.97	Gly	0.00	Ser	-0.53
Phe	-0.95	Phe	0.06	Asp$^-$	-0.42
Val	-0.83	Trp	0.06	Cys	-0.42
Thr	-0.56	Cys	0.12	Asn	-0.39
Gly	0.00	Tyr	0.90	Gly	0.00
Pro	+3.00	Pro	1.51	Pro	2.50

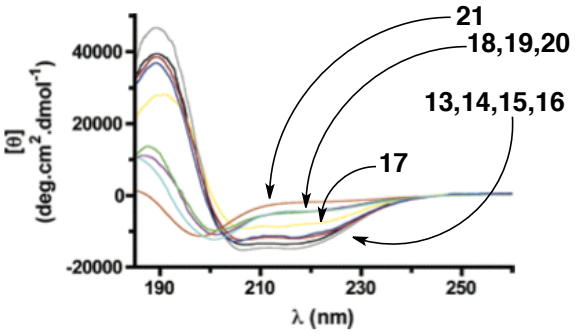

Figure 3. CD spectra of compounds **13** (black), **14** (grey), **15** (red), **16** (blue), **17** (yellow), **18** (purple), **19** (green), **20** (aqua), and **21** (orange) in 10 mM phosphate buffer (pH 7.4, 25 °C).

ref. CD spectra-1

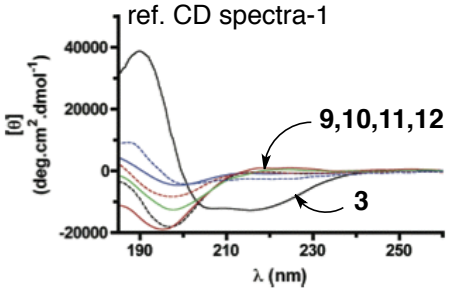

Figure 7. CD spectra of compounds **3** (black, solid), **9** (black, broken), **10** (red, solid), **11** (blue, solid), and **12** (green, solid) in 10 mM phosphate buffer (pH 7.4, 25 °C); **10** (red, broken) in 0.01 M HCl (pH 2) and **11** (blue, broken) in 0.001 M NaOH (pH 11).

3-2-4 NMR analysis of short peptides

A low temperature dependence for amide NH chemical shifts (values ≤4ppb/K) are indicative of hydrogen bonds.

13 Ac-(cyclo-2,6)-R[KAAAD]

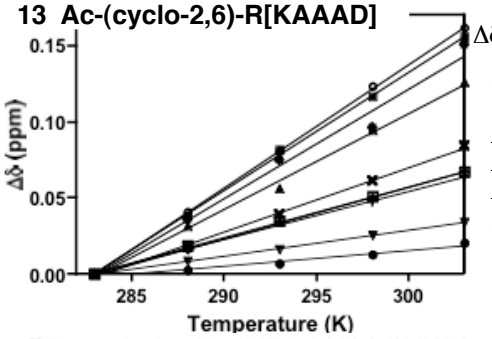

Figure S5. Temperature dependence of the amide NH chemical shifts for **13** in H_2O/D_2O (9:1). Line slopes indicating temperature coefficients (Δδ/T) for each residue are shown (in brackets) ■ Arg1 (8 ppb/K), ▲ Lys2 (6 ppb/K), ▼ Ala3 (2 ppb/K), ◆ Ala4 (3 ppb/K), ● Ala5 (1 ppb/K), ✖ Asp6 (4 ppb/K), □ Terminal NH1 (3 ppb/K), ○ Terminal NH2 (8 ppb/K), ✚ Arg1 side chain NH (3 ppb/K), ✳ Lys2 side chain NH (7 ppb/K), values ≤ 4 are indicative of hydrogen bonds.

Δδ/T of each residue NH

Arg1 8ppb/K
Lys2 6ppb/K
Ala3 2ppb/K
Ala4 3ppb/K
Ala5 1ppb/K
Asp6 4ppb/K
NH1 3ppb/K
NH2 8ppb/K

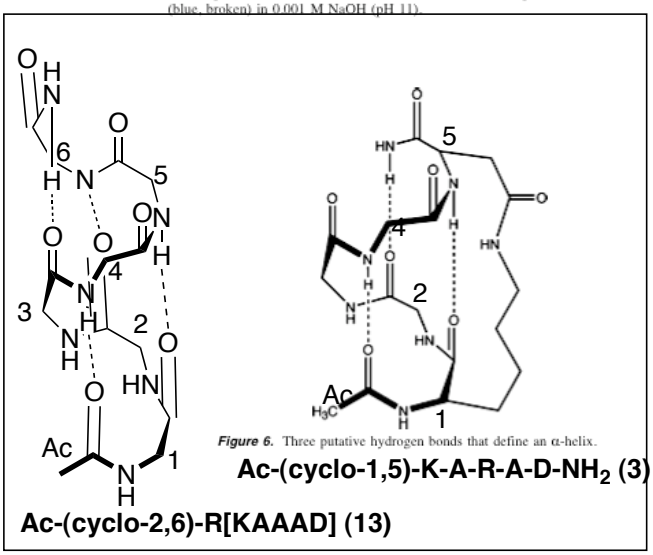

Figure 6. Three putative hydrogen bonds that define an α-helix.

The NMR analysis indicated the presence of three hydrogen bonds within the pentapeptide.

Temperature effect to the stability of **3**

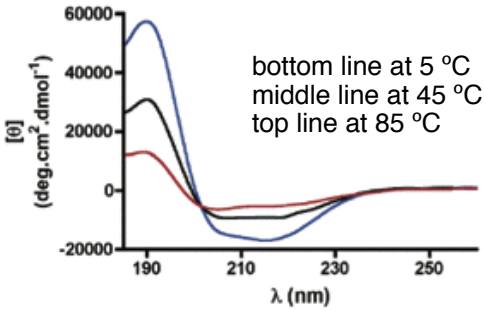

Gua. HCl (protein denaturant) effect to the stability of **3**

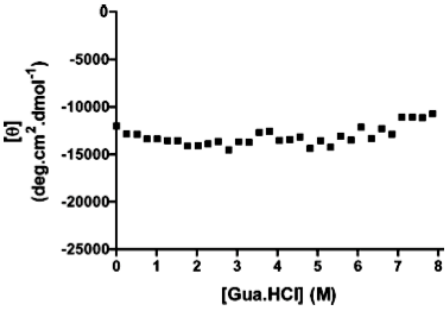

Figure 9. Variation in molar elipticity of **3** at 215 nm with increasing [guanidine• HCl] at 25 °C.

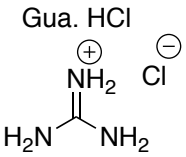

3-3 biological activity of lactam linking peptides

ideal; parent peptide ⟹ *cross-linking* alpha helicity↑, biological activity↑

example 1 (A. M. Felix et al. Biopolymers, 1995, 37,67)

GRF; growth hormone-releasing factor (Nature, 1982, 300, 276)

human-GRF [1] [5] [10] [15] [20] [25] [30] [35] [40] [44]
Y A D A I F T N S Y R K V L G Q L S A R K L L Q D I M S R Q Q G E S N Q E R G A R A R L -

Table V Biological Activity of Cyclic hGRF(1–29)-NH_2 ($hGRF_{29}$) Analogues

Type	hGRF Analogue	Relative Potency[a]
Linear	hGRF(1–44)-NH_2	1.00
	[Ala^{15}]-$hGRF_{29}$	3.81
$i-(i+9)$	Cyclo(Asp^{3}-Lys^{12})-[Ala^{15}]-$hGRF_{29}$	0.07
$i-(i+5)$	Cyclo(Lys^{11}-Glu^{16})-[Ala^{15}]-$hGRF_{29}$	0.02
$i-(i+5)$	Cyclo(Glu^{16}-Lys^{21})-[Ala^{15}]-$hGRF_{29}$	0.02
$i-(i+4)$	Cyclo(Lys^{4}-Asp^{8})-[Ala^{15}]-$hGRF_{29}$	1.58
	Cyclo(Asp^{8}-Lys^{12})-[Ala^{15}]-$hGRF_{29}$ **(A)**	0.77
	Cyclo(Lys^{12}-Glu^{16})-[Ala^{15}]-$hGRF_{29}$	0.80
	Cyclo(Glu^{16}-Lys^{20})-[Ala^{15}]-$hGRF_{29}$	0.24
	Cyclo(Lys^{21}-Asp^{25})-[Ala^{15}]-$hGRF_{29}$ **(B)**	1.33
	Cyclo(Asp^{8}-Lys^{12})-[$desNH_2Tyr^{1}$, D-Ala^{2}, Ala^{15}]-$hGRF_{29}$	2.47
	Cyclo(Lys^{21}-Asp^{25})-[$desNH_2Tyr^{1}$, D-Ala^{2}, Ala^{15}]-$hGRF_{29}$	1.33
Multiple	Dicyclo(Asp^{8}-Lys^{12})(Glu^{16}-Lys^{20})-[Ala^{15}]-$hGRF_{29}$ **(C)**	0.02
$i-(i=4)$	Dicyclo(Glu^{16}-Lys^{20})(Lys^{21}-Asp^{25})-[Ala^{15}]-$hGRF_{29}$	0.02
	Dicyclo(Lys^{12}-Glu^{16})(Lys^{21}-Asp^{25})-[Ala^{15}]-$hGRF_{29}$	0.23
	Dicyclo(Asp^{8}-Lys^{12})(Lys^{21}-Asp^{25})-[Ala^{15}]-$hGRF_{29}$	0.69
	Dicyclo(Asp^{8}-Lys^{12})(Lys^{21}-Asp^{25})-[$desNH_2Tyr^{1}$, D-Ala^{2}, Ala^{15}]-$hGRF_{29}$	2.81
	Dicyclo(Asp^{8}-[Gly]-Orn^{12})(Orn^{21}-[Gly]-Asp^{25})-[Ala^{15}]-$hGRF_{29}$	4.36

[a] GH-releasing potency relative to hGRF(1–44)-NH_2; determined using cultured rat pituitary cells exposed to 3.1 → 400 pM hGRF analogue for 4 h, 37°C.

(hGRF1-29; 0.8
ref. I. J.Pept. Protein. Res)

CD measurements of [Ala^{15}]-$hGRF_{29}$ show a slight increase in alpha helicity relative to the parent peptide .
ref. Proc. 10th American Peptide Symposium (G. Marshall ed. p.465)

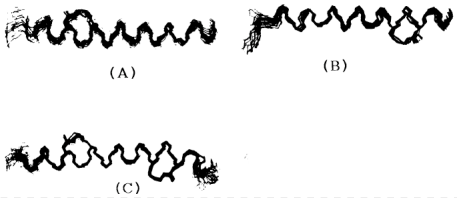

FIGURE 4 Superposition of structures of the GRF analogues obtained from evaluation of the nmr data in 75% methanol, pH 6.0, by constrained dynamics and minimization calculations. Structures are oriented with the N-terminus toward the left. (A) Cyclo(Asp^{8}-Lys^{12})-[Ala^{15}]-hGRF(1–29)-NH_2. (B) Cyclo(Lys^{21}-Asp^{25})-[Ala^{15}]-hGRF(1–29)-NH_2. (C) Dicyclo(Asp^{8}-Lys^{12})(Lys^{21}-Asp^{25})-[Ala^{15}]-hGRF(1–29)-NH_2.

example 2 Bcl-2-BakBH3 (regulation of apoptosis)
B. Yang et al. Bioorg.Chem. Lett. 2004, 14, 1403

Table 1. Lactam-bridged cyclic BakBH3 peptides

Peptides	Sequences	% Helix (in PBS)
Bak BH3	GQVGRQLAIIGDDINR (1 5 10 15)	14[a]
LB1	GQVGRQLAKIGDDINR	35
LB2	GQVGRQLKIIGDDINR	41
LB3	GQVGKQLAEIGDDINR	78
LB4	GQVGRQLAIIGDDINK	56

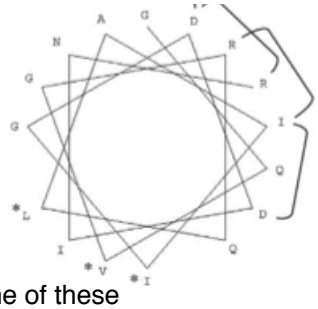

none of these
lactam cross-linking peptides
showed any binding to Bcl-2.
(Data were not shown in this paper.)

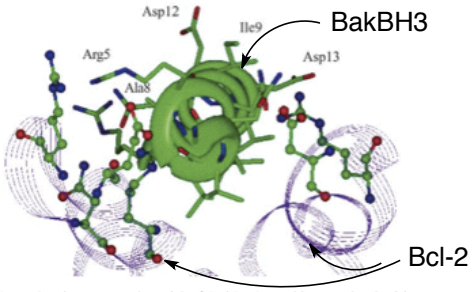

Figure 3. The structural model of BakBH3 peptide completed with Bcl-2 which is built based on the NMR structure of this peptide and Bcl-x_L[2]. The residues or positions that are used for the lactam bridge formation are shown.

4 cross-linking with an all hydrocarbon staple

Gregory L. Verdine et al. JACS, 2000, 122, 5891

4-1 design

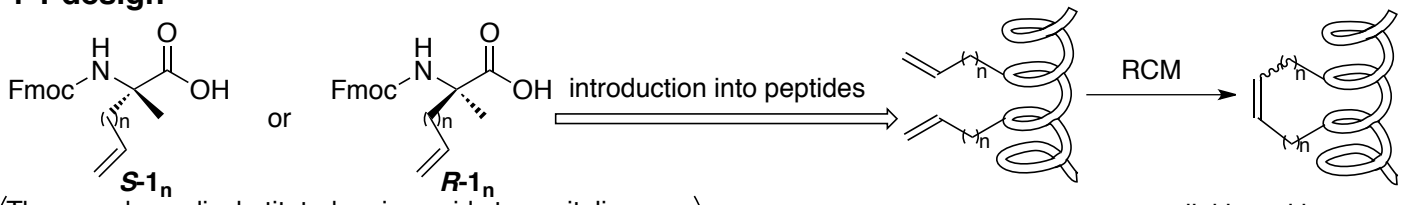

They used α,α-disubstituted amino acids to capitalize on the helix-stabilizing effect of them.
α helices; $\phi \approx -60^o$, $\psi \approx -40^o$
α,α-disubstituted amino acids; $\phi \approx -60 \pm 20^o$, $\psi \approx -30 \pm 20^o$

4-2 synthesis

The actual structure of cross-links is dependent on the stereochemistry at the attachment points.

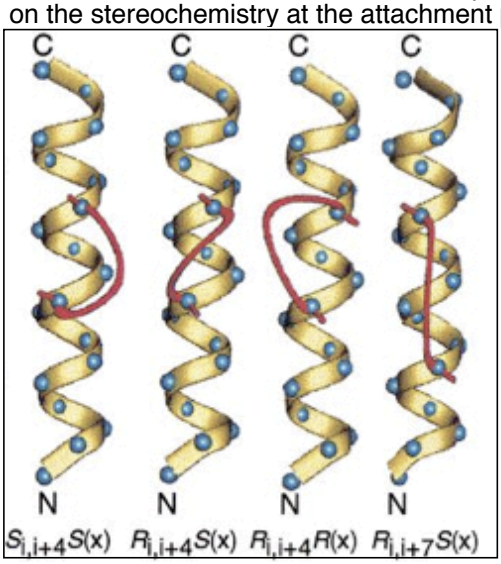

synthesis of ***S*-1** and ***R*-1**

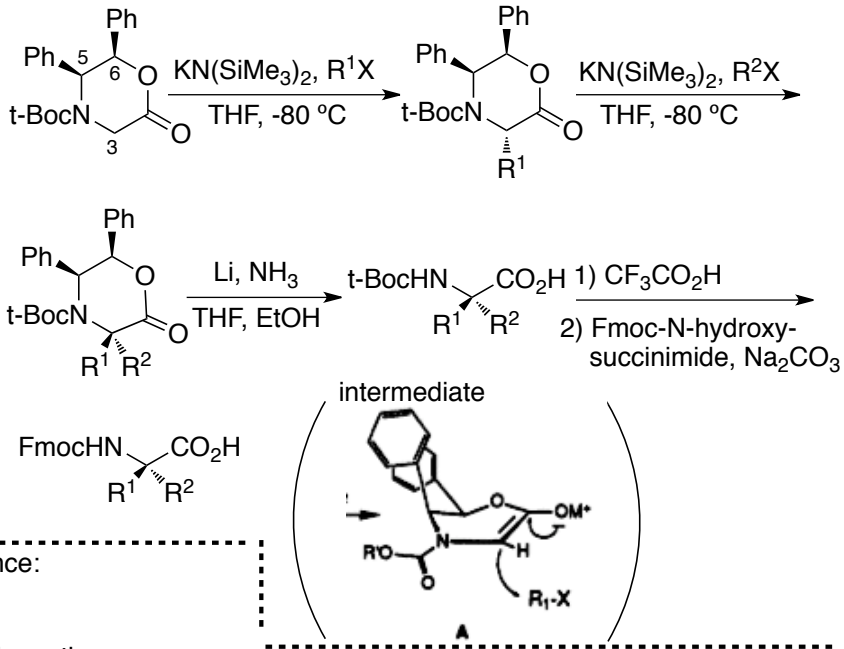

• The wild-type peptide (RNAse A) has the sequence:
Ac-EWAETAAAKFLAAHA-NH_2

• The peptides synthesized in the $R_{i,i+7}S(x)$ series have the sequences:
Ac-EWAE***y***AAAKFL***z***AHA-NH_2 where (***y,z***) were substituted with (***R-1₃,S-1₃***), (***R-1₃,S-1₄***), (***R-1₄,S-1₄***), (***R-1₃,S-1₆***), (***R-1₄,S-1₆***) for the peptides ***R*$_{i,i+7}$*S(8)***, ***R*$_{i,i+7}$*S(9)***, ***R*$_{i,i+7}$*S(10)***, ***R*$_{i,i+7}$*S(11)***, and***R*$_{i,i+7}$*S(12),*** respectively.

• The peptides synthesized in the $S_{i,i+4}S(x)$, $R_{i,i+4}R(x)$ and $R_{i,i+4}S(x)$ series have the sequences:
Ac-EWAETAA***y***KFL***z***AHA-NH_2 where (***y,z***) were substituted with (***S-1₁,S-1₃***), (***S-1₁,S-1₄***), (***S-1₃,S-1₃***), (***R-1₁,R-1₃***), (***R-1₁,S-1₂***), (***R-1₁,S-1₃***) and (***R-1₁,S-1₄***)for the peptides ***S*$_{i,i+4}$*S(6)***, ***S*$_{i,i+4}$*S(7)***, ***S*$_{i,i+4}$*S(8)***, ***R*$_{i,i+4}$*R(6)***, ***R*$_{i,i+4}$*R(7)***, ***R*$_{i,i+4}$*R(8)***, ***R*$_{i,i+4}$*S(5)***, ***R*$_{i,i+4}$*S(6)***, and***R*$_{i,i+4}$*S(7),*** respectively.

Metathesis reaction

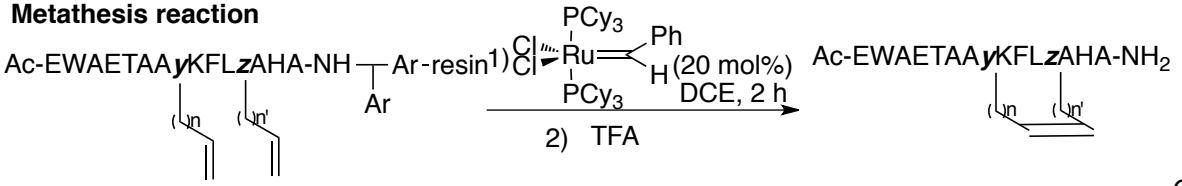

percent conversion product / product+starting material (determined by HPLC)

cross-link	% conversion[a]	cross-link	% conversion[a]	cross-link	% conversion[a]
$R_{i,i+7}S(8)$	0	$S_{i,i+4}S(6)$	0	$R_{i,i+4}R(6)$	0
$R_{i,i+7}S(9)$	51	$S_{i,i+4}S(7)$	68	$R_{i,i+4}R(7)$	17
$R_{i,i+7}S(10)$	77	$S_{i,i+4}S(8)$	>98	$R_{i,i+4}R(8)$	>98
$R_{i,i+7}S(11)$	>98				
$R_{i,i+7}S(12)$	>98				

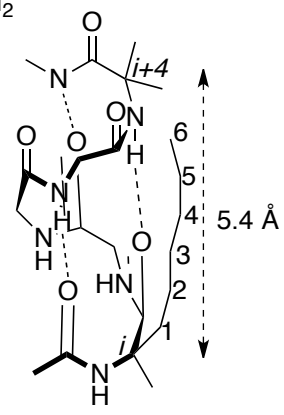

4-3 result

Percent helix

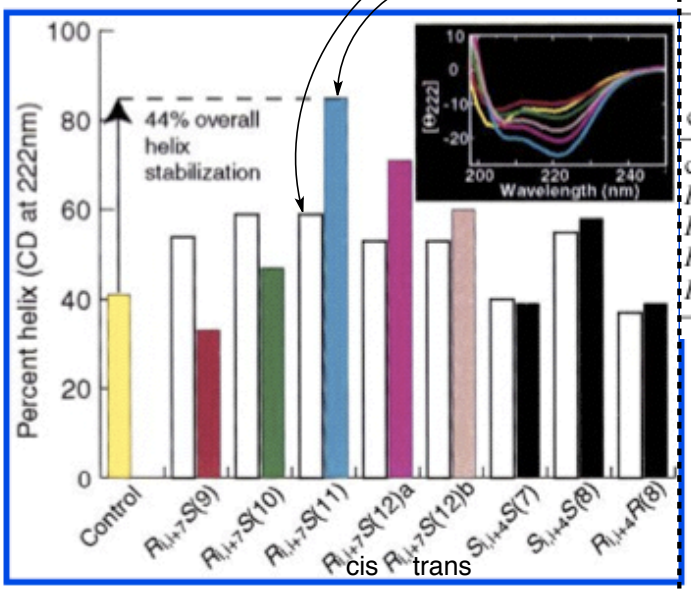

cleavage by trypsin (protease resistance *in vitro*)

cross-link	cleavage rate constant (M^{-1} s^{-1}) unmetathesized	metathesized and hydrogenated
control	2.39	
$R_{i,i+7}S(9)$		0.37
$R_{i,i+7}S(10)$		0.34
$R_{i,i+7}S(11)$	0.50	0.058
$R_{i,i+7}S(12)$		0.12

$R_{i,i+7}S(x)$ = Ac-EWAEyAAA**K**FLzAHA-NH_2

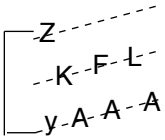

4-4 biological activity of α helics peptide stabilized by a hydrocarbon staple

Gregory L. Verdine et al. Science, 2004, 305, 1466

Bcl-2 (B-cell lymphoma 2) proteins constitute a critical control point for the regulation of apoptosis.
BID is a pro-apptotic protein that, in response to death receptor signaling, interconnects the extrinsec and core intrinsic apoptotic pathways. Activated BID can bind to BCL-2 and trigger activation of pro-apoptotic proteins, resulting in cytochrome c release.

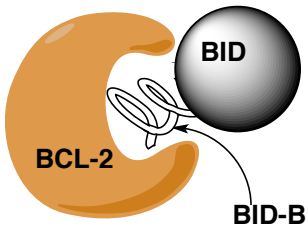

cytochrome c release → apoptosis

BID-BH3 (23 amino acid residues)

B

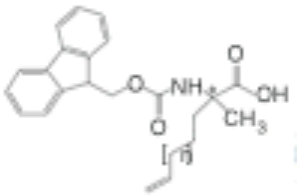

n=1: S5,R5
n=4: S8

Compound	1 5 10 15 20	
BID BH3	EDIIRNIARHLAQVGDSN$_L$DRSIW	
$SAHB_A$	EDIIRNIARHLA*VGD*N$_L$DRSIW	$S_{i,i+4}S(8)$
$SAHB_{A\,(G\rightarrow E)}$	EDIIRNIARHLA*VED*N$_L$DRSIW	$S_{i,i+4}S(8)$
$SAHB_B$	EDIIRNI*RHL*QVGDSN$_L$DRSIW	$S_{i,i+4}S(8)$
$SAHB_C$	EDIIRNIA*HLA*VGDSN$_L$DRSIW	$S_{i,i+4}S(8)$
$SAHB_D$	EDIIRNIAR*LAQVGD*N$_L$DRSIW	$R_{i,i+7}S(11)$

*=S5, *=R5, *=S8, N_L=norleu

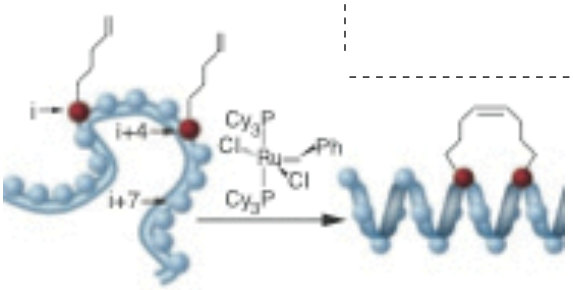

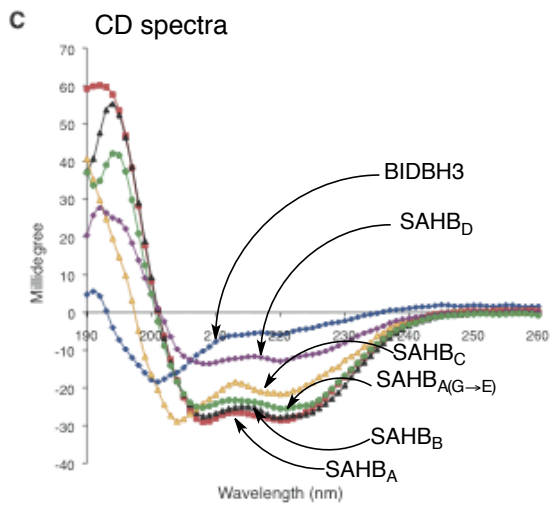

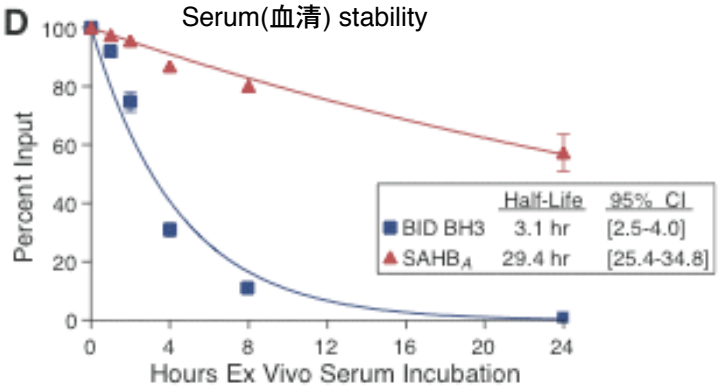

Serum includes all proteins not used in blood clotting and all the electrolytes, antibodies, antigens, hormones, and any exogenous substances (e.g., drugs and microorganisms).

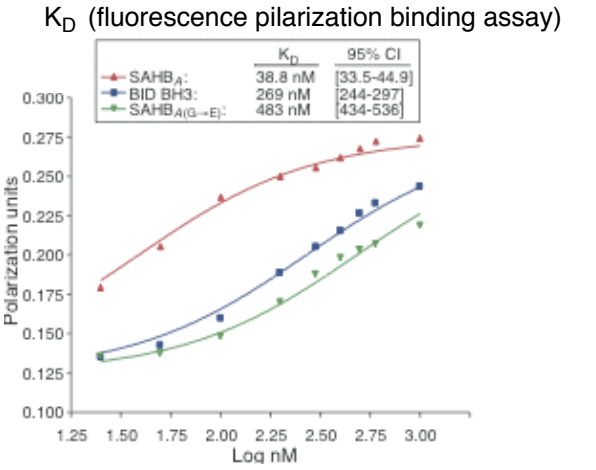

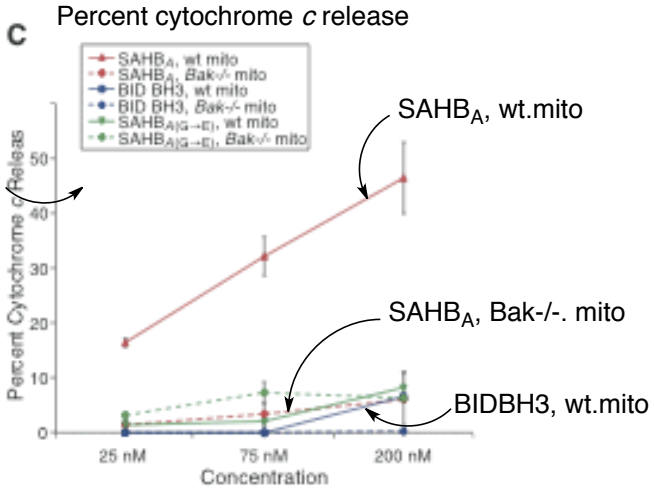

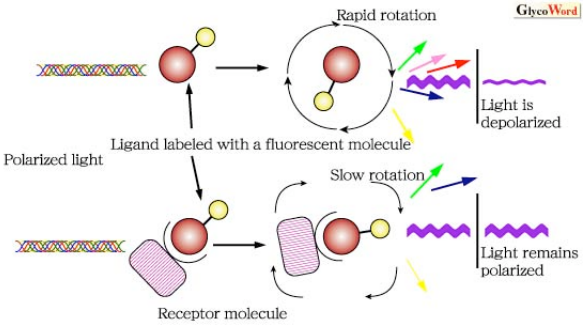

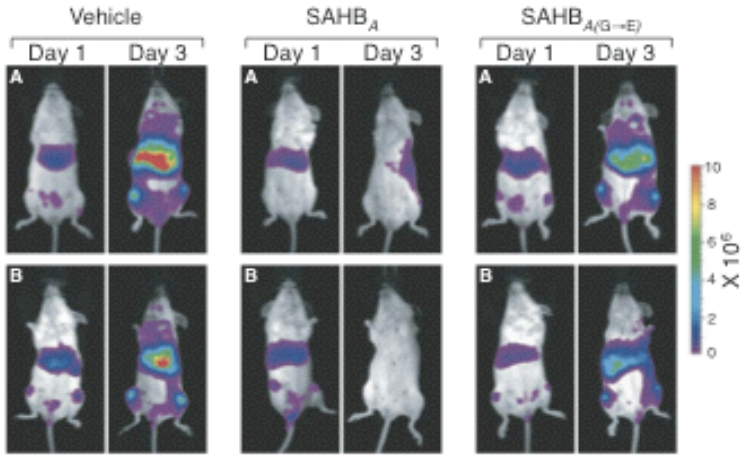

intravenous injection (静注) leukemia cells that stably expressed luciferase

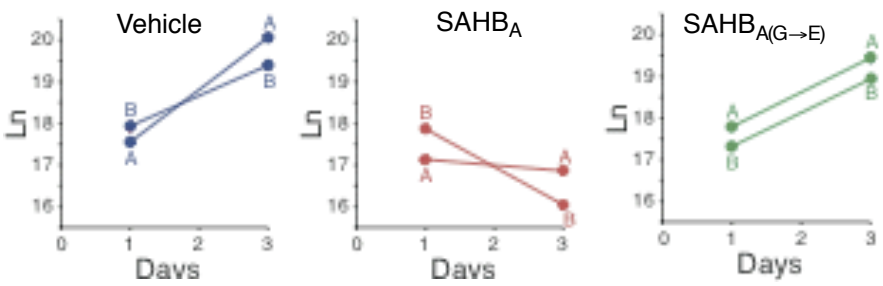

4-5 the physical forces that underlie stapled peptide stabilization

Gregory L. Verdine and Eugene I. Shakhnovich et al. JACS, 2009, 131, 4622

Why some cases (RNAse A) an *i, i+7* staple can be more stabilizing than an *i,i+4* staple, while in other cases (BIDBH3) the opposite is true?
What factors are most important?

$H = E_{con} + w_{hb}E_{hb} + w_{bbtor}E_{bbtor} + w_{sct}E_{sct} + w_{linktor}E_{linktor}$

E_{con}; intermolecular potencial energy
E_{hb}; hydrogen-bonding potential
E_{bbtor}; sequence-dependent backbone torsional potential
E_{sct}; side-chain torsional angle potential
$E_{linktor}$; torsional potential for hydrocarbon linker

S = configurational entropy of the peptide + that of the staple

Four variables in E_{bbtor} function are ϕ_{A+1},ψ_{A+1}, the angle between b_{Ai} and b_{Ai+2} and the angle between P_{Ai} and P_{Ai+2}.

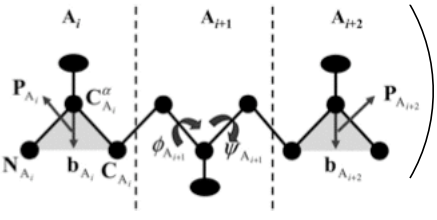

	Compound	Sequence
RNAse A	WT	EWAETAAAKFLAAHA
	i,i+4 staple	EWAETAA*KFL*AHA
	i,i+7 staple	EWAE*AAAKFL*AHA
	i,i+7 Ala	EWAEAAAAKFLAAHA
BID BH3	WT	EDIIRNIARHLAQVGDSMDRSIW
	SAHB A *i,i*+4 staple	EDIIRNIARHLA*VGD*MDRSIW
	i,i+4 Ala	EDIIRNIARHLAAVGDAMDRSIW
	SAHB D *i,i*+7 staple	EDIIRNIAR*LAQVGD*MDRSIW
	i,i+7 Ala	EDIIRNIARALAQVGDAMDRSIW

Conformations that were obtained during MC simulations

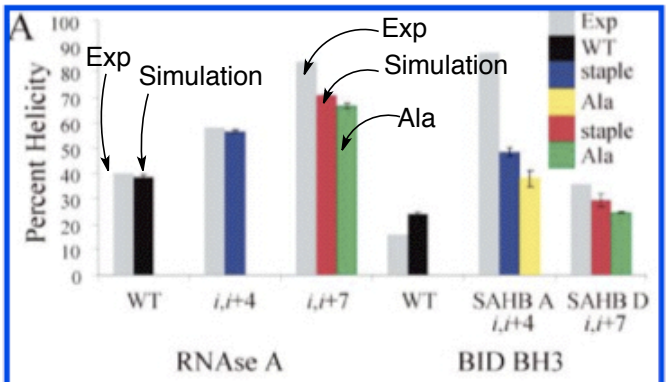

Their simulation was able to predict which staple would be more stabilizing for each peptide.

In all cases, the stapled peptides are more helical than the corresponding alanine-substituted versions, suggsting that the physical constraint conferred by macrocyclic ring formation contributes to increased helical propensity.

Table 1. Thermodynamic Analysis of RNAse A and BID BH3 Simulations Using the Number of Helical Residues as the Order Parameter

	ΔH	$-T\Delta S$	ΔG	$\Delta\Delta H$	$-T\Delta\Delta S$	$\Delta\Delta G$
			RNase A			
WT	-29.2 ± 0.6	32.5 ± 0.6	3.3 ± 0.1			
i,i+4 staple	-30.0 ± 0.5	31.9 ± 0.4	1.9 ± 0.1	-0.8 ± 0.5	-0.6 ± 0.5	-1.37 ± 0.07
i,i+7 staple	-33.25 ± 0.06	33.4 ± 0.1	0.12 ± 0.09	-4.0 ± 0.6	0.9 ± 0.5	-3.14 ± 0.07
i,i+7 Ala	-32.59 ± 0.09	34.16 ± 0.09	1.57 ± 0.04	-3.4 ± 0.5	1.7 ± 0.5	-1.7 ± 0.2
			BID BH3			
WT	-47.0 ± 0.4	48.2 ± 0.4	1.2 ± 0.1			
i,i+4 staple	-48.3 ± 0.3	47.7 ± 0.3	-0.63 ± 0.03	-1.4 ± 0.5	-0.5 ± 0.4	-1.8 ± 0.1
i,i+4 Ala	-49.2 ± 0.4	49.0 ± 0.5	-0.16 ± 0.04	-2.2 ± 0.3	0.8 ± 0.4	-1.4 ± 0.1
i,i+7 staple	-47.5 ± 0.2	48.0 ± 0.1	0.56 ± 0.05	-0.5 ± 0.5	-0.1 ± 0.5	-0.7 ± 0.1
i,i+7 Ala	-46.5 ± 0.4	47.9 ± 0.3	1.38 ± 0.04	0.4 ± 0.5	-0.2 ± 0.4	0.2 ± 0.1

[a] The temperatures used for RNase A and BID BH3 were 0.78 and 0.70, respectively. Errors are reported as standard deviations of averages of three groups of 50 runs (RNase A) or 200 runs (BID BH3). Thermodynamic values for folding to the helical state (ΔH, ΔS, ΔG) are given, as well as these values relative to the WT peptide ($\Delta\Delta H$, $\Delta\Delta S$, $\Delta\Delta G$).

For all stapled peptides ΔΔH makes a larger contribution to ΔΔG than -TΔΔS.

Table S2. Contributions of each potential term to overall enthalpic change ΔH for folding to the helical state, as well as the enthalpic change relative to the WT peptide $\Delta\Delta H$.

		WT	*i,i*+4 staple	*i,i*+4 Ala	*i,i*+7 staple	*i,i*+7 Ala
RNAse A	ΔH^a	-29.2_ ± 0.6_	-30.0_ ± 0.5_		-33.25 ± 0.06	-32.59 ± 0.09
	ΔH(con)	-1.05 ± 0.05	-0.75 ± 0.08		-0.37 ± 0.02	-0.57 ± 0.07
	ΔH(hb)	-11.4_ ± 0.5_	-11.9_ ± 0.1_		-14.03 ± 0.07	-13.9_ ± 0.1_
	ΔH(bbtor)	-16.76 ± 0.09	-17.3_ ± 0.3_		-18.50 ± 0.09	-17.83 ± 0.09
	ΔH(sct)	0.0_ ± 0.3_	-0.14 ± 0.09		-0.28 ± 0.04	-0.2_ ± 0.1_
	ΔH(linktor)		0.1_ ± 0.1_		-0.07 ± 0.09	
	$\Delta\Delta H^a$		-0.8_ ± 0.5_		-4.0_ ± 0.6_	-3.4_ ± 0.5_
	$\Delta\Delta H$(con)		0.3_ ± 0.1_		0.69 ± 0.05	0.49 ± 0.06
	$\Delta\Delta H$(hb)		-0.5_ ± 0.4_		-2.7_ ± 0.5_	-2.6_ ± 0.6_
	$\Delta\Delta H$(bbtor)		-0.6_ ± 0.4_		-1.7_ ± 0.2_	-1.1_ ± 0.2_
	$\Delta\Delta H$(sct)		-0.1_ ± 0.4_		-0.3_ ± 0.3_	-0.2_ ± 0.2_
	$\Delta\Delta H$(linktor)		0.1_ ± 0.1_		-0.07 ± 0.09	
BID BH3	ΔH^a	-47.0_ ± 0.4_	-48.3_ ± 0.3_	-49.2_ ± 0.4_	-47.5_ ± 0.2_	-46.5_ ± 0.4_
	ΔH(con)	-0.3_ ± 0.1_	-0.43 ± 0.07	-0.5_ ± 0.1_	-0.4_ ± 0.1_	-0.6_ ± 0.1_
	ΔH(hb)	-24.3_ ± 0.2_	-24.85 ± 0.09	-24.9_ ± 0.1_	-23.20 ± 0.1_	-22.7_ ± 0.1_
	ΔH(bbtor)	-22.6_ ± 0.2_	-23.3_ ± 0.3_	-23.6_ ± 0.1_	-24.0_ ± 0.2_	-23.9_ ± 0.2_
	ΔH(sct)	0.2_ ± 0.2_	0.2_ ± 0.2_	-0.2_ ± 0.3_	0.41 ± 0.07	0.7_ ± 0.4_
	ΔH(linktor)		-0.01 ± 0.02		-0.25 ± 0.05	
	$\Delta\Delta H^a$		-1.4_ ± 0.5_	-2.2_ ± 0.3_	-0.5_ ± 0.5_	0.4_ ± 0.5_
	$\Delta\Delta H$(con)		-0.2_ ± 0.1_	-0.19 ± 0.03	-0.16 ± 0.09	-0.36 ± 0.04
	$\Delta\Delta H$(hb)		-0.6_ ± 0.2_	-0.6_ ± 0.4_	1.1_ ± 0.1_	1.6_ ± 0.1_
	$\Delta\Delta H$(bbtor)		-0.6_ ± 0.4_	-1.0_ ± 0.3_	-1.4_ ± 0.3_	-1.3_ ± 0.3_
	$\Delta\Delta H$(sct)		0.0_ ± 0.2_	-0.4_ ± 0.3_	0.2_ ± 0.2_	0.5_ ± 0.5_
	$\Delta\Delta H$(linktor)		-0.01 ± 0.02		-0.25 ± 0.05	

5 cross-linking with acetylenic cross-linking agent

M. Inouye et al. Chem Comm, 2004, 1280
M. Inouye et al. Chem. Eur. J. 2008, 14, 857
G. A Wooley et al. JACS. 2007, 129, 14154

5-1 design

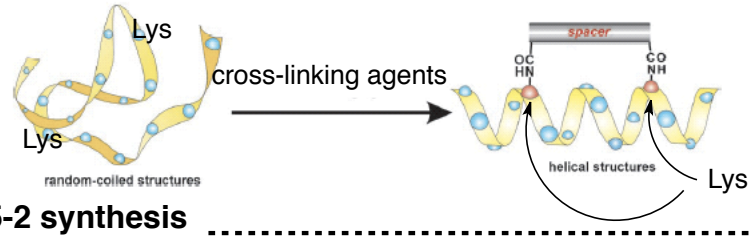

5-2 synthesis

A : Ac-Ala-Ala-Glu-Ala-Glu-Ala-Ala-Trp-Ala-Lys-Ala-Glu-Ala-Lys-Glu-Ala-NH$_2$ (*i*+4, *i*)

B : Ac-Ala-Ala-Glu-Ala-Trp-Ala-Lys-Ala-Glu-Ala-Ala-Glu-Ala-Lys-Glu-Ala-NH$_2$ (*i*+7, *i*)

solid phase peptide synthesis using the standard Fmoc chemistry

NH-resin —(Fmoc-Ala-OH, BOP reagent)→ Fmoc-Ala-NH-resin —(piperidine)→ H_2N-Ala-NH-resin —(Fmoc-Glu(PG)-OH, BOP reagent)→ H_2N-Glu(PG)-Ala-resin

→ Fmoc-Ala-Ala-Glu(PG)-Ala-Trp-Ala-Lys(PG)-Ala-Glu(PG)-Ala-Ala-Glu(PG)-Ala-Lys(PG)-Glu(PG)-Ala-resin

(1) piperidine, (2) Ac_2O → Ac-Ala-Ala-Glu(PG)-Ala-Trp-Ala-Lys(PG)-Ala-Glu(PG)-Ala-Ala-Glu(PG)-Ala-Lys(PG)-Glu(PG)-Ala-resin

TFA → Ac-Ala-Ala-Glu-Ala-Trp-Ala-Lys-Ala-Glu-Ala-Ala-Glu-Ala-Lys-Glu-Ala-NH_2 —(cross-linking agent, buffer)→

Ac-Ala-Ala-Glu-Ala-Trp-Ala-Lys-Ala-Glu-Ala-Ala-Glu-Ala-Lys-Glu-Ala-NH_2

cross-linking agent

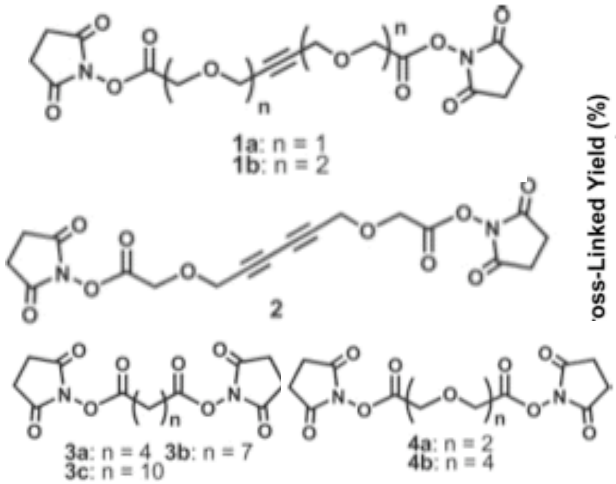

cross-linking yield

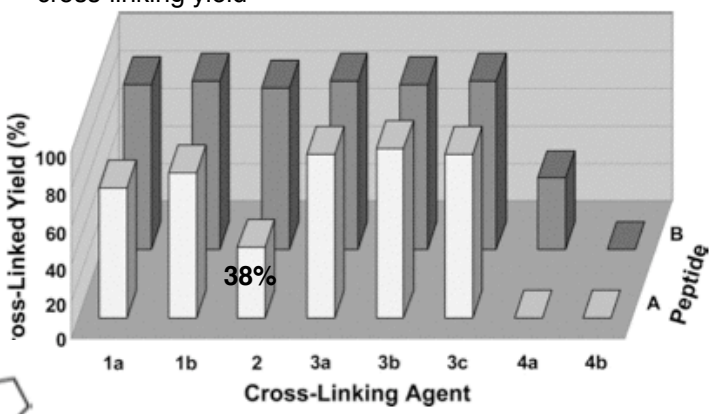

Fig. 2 The yields of the cross-linked peptides after 60 min.

5-3 result

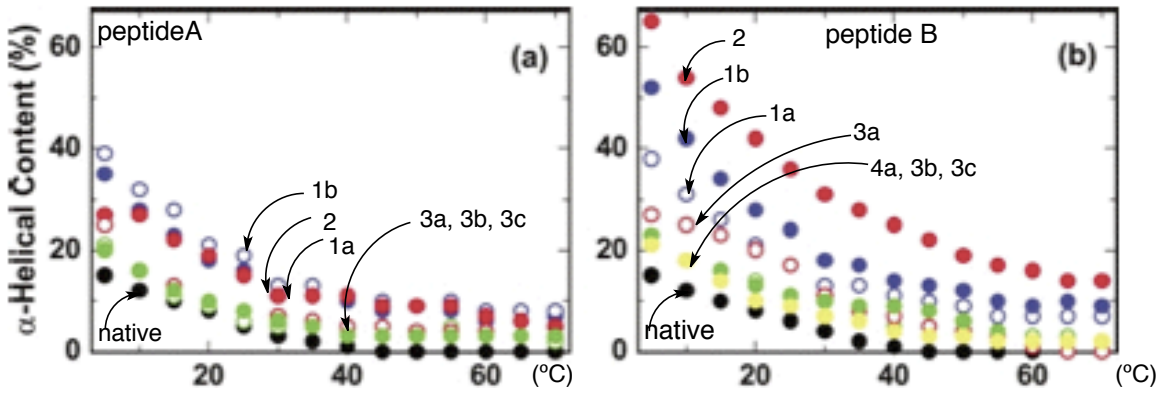

peptide B (Lys→X); Ac-Ala-Ala-Glu-Ala-Trp-Ala-X-Ala-Glu-Ala-Ala-Glu-Ala-X-Glu-Ala-NH_2

Other cross-linking agents

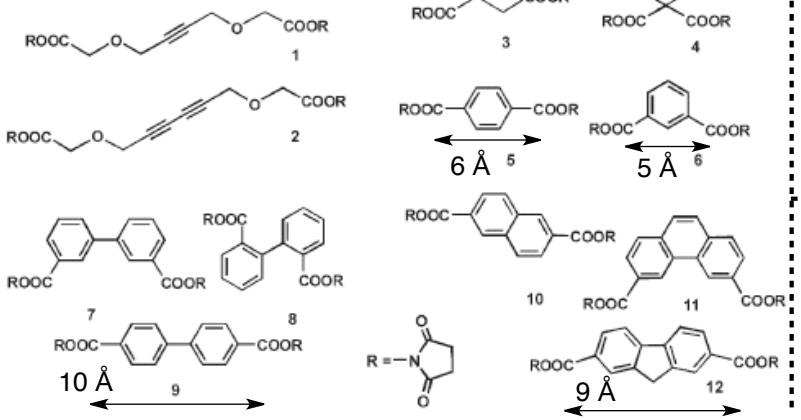

X residues

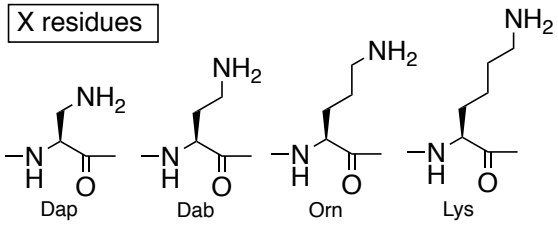

Figure 3. Cross-linking agents: acetylenic **1** and **2**, short alkylene-based **3** and **4**, benzene-based **5** and **6**, biphenylene-based **7–9**, and highly rigid **10–12**.

helical content

Peptides **B** (*i*/*i*+7: 1.1 nm)

CL-agent	X = Dap	Dab	Orn	Lys
1	–	–	–	~35
2	–	–	–	~65
3	–	L (L)	H (M)	M (L)
4	–	L (L)	L (L)	M (M)
5	L (L)	M (L)	80 (60)	H (M)
6	–	90 (60)	85 (60)	H (M)
7	–	H (M)	H (M)	H (M)
8	–	M (L)	M (M)	H (M)
9	–	L (L)	L (L)	L (L)
10	–	L (L)	M (L)	M (L)
11	–	M (L)	M (M)	H (M)
12	–	L (L)	L (L)	L (L)

H = 40-60%, M = 20-40%, L = 0-20%

Reversible photoregulation of helical structure in short peptides (M. Inouye et al. Org. Lett. 2006, 8, 285)

Isomerization of the spiropyran to the merocyanine

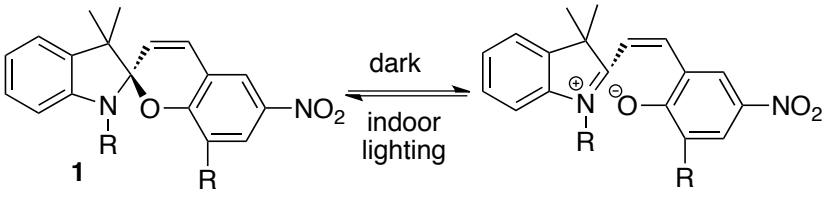

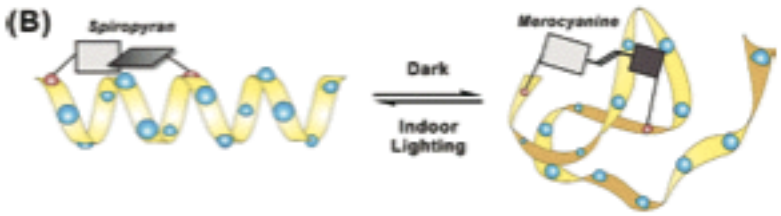

R = $(CH_2)_2CO_2$N

photochromic features of spiropyran skeltons

1) only merocyanine forms strongly absorb visible light
2) mericyanines are more stable than the spiropyrans in aqueous media under dark conditions
3) [merocyanine]/[spiropyran] = 1.13 (dark)
   = 0.01 (light)

Scheme 1. Synthetic Route for **1**

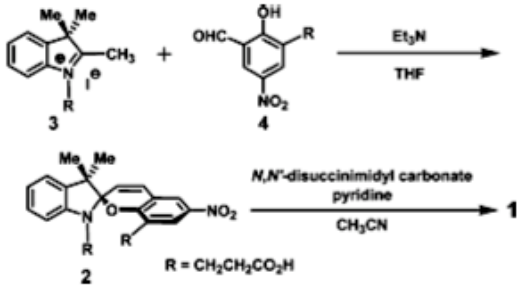

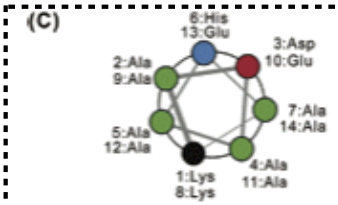

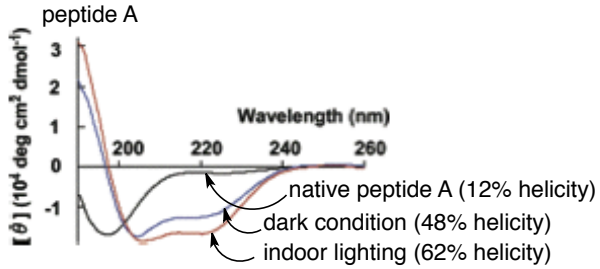

Figure 2. CD spectra of the native peptide A (black) and the cross-linked peptide **A·1** under indoor lighting (red) and dark (blue) conditions in 100 mM phosphate buffer (pH 6.6) at 25 °C using a 1 mm cell.

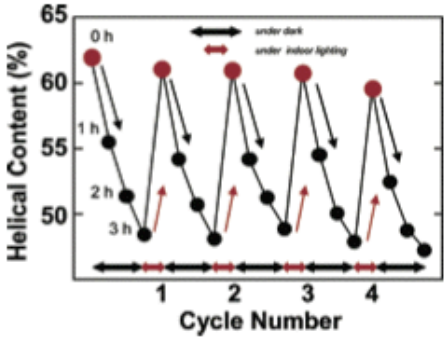

Figure 3. Switching behavior for the helical contents of the dark-adapted **A·1** under the same conditions described in text. Red circles correspond to the helical contents after exposure of **A·1** to indoor lighting for 20 min.